



Conformal poly(ethyl α -cyanoacrylate) nano-coating for improving the interface stability of $\text{LiNi}_{0.5}\text{Mn}_{1.5}\text{O}_4$



Zhaolin Liu^{a,b,1}, Pu Hu^{b,c,1}, Jun Ma^b, Bingsheng Qin^b, Zhongyi Zhang^{a,*}, Chunbo Mou^a, Yan Yao^c, Guanglei Cui^{b,*}

^a Qingdao University, Qingdao, 266071, PR China

^b Qingdao Industrial Energy Storage Research Institute, Qingdao Institute of Bioenergy and Bioprocess Technology, Chinese Academy of Sciences, Qingdao, 266101, PR China

^c Department of Electrical and Computer Engineering and Materials Science and Engineering Program, University of Houston, Houston, TX 77204, USA

ARTICLE INFO

Article history:

Received 20 January 2017

Received in revised form 13 March 2017

Accepted 22 March 2017

Available online 24 March 2017

Keywords:

Lithium-ion battery

Interface

Conformal coating

Polymer electrolyte

High voltage cathode

ABSTRACT

Undesired interfacial reaction between the high voltage spinel $\text{LiNi}_{0.5}\text{Mn}_{1.5}\text{O}_4$ and commercial organic electrolyte is one of the most essential obstacles for the application of cathode material $\text{LiNi}_{0.5}\text{Mn}_{1.5}\text{O}_4$ in lithium-ion batteries (LIBs). Here, to amend the high voltage cathode/electrolyte interface of $\text{LiNi}_{0.5}\text{Mn}_{1.5}\text{O}_4$, we proposed a conformal nano-coating strategy by in-situ polymerization of poly(ethyl α -cyanoacrylate) (PECA) on its surface. The electrochemical measurement results demonstrated that the conformal PECA nano-coating film, acting as high voltage polymer electrolyte, transition metallic ions blocking layer, and buffer layer against electrolyte erosion and particle cracks, can successfully decrease polarization and enhance capacity retention during cycling of $\text{LiNi}_{0.5}\text{Mn}_{1.5}\text{O}_4$. This work will inspire extensive and intensive research on the interface modification of LIBs.

© 2017 Elsevier Ltd. All rights reserved.

1. Introduction

As the primary power supply of portable equipment, lithium-ion batteries (LIBs) have recently attracted great attention for applications in electric vehicles and large-scale energy storage systems [1–4]. In order to satisfy the demands of these applications, it is urgently required to further improve energy and power densities and resolve the issues of safety and lifetime. As the energy density of a battery is defined by its capacity and voltage, enhancement in voltage is the appropriate approach to increasing the cell energy density [5–11]. Although 4 V-class cathodes (LiMn_2O_4 , LiCoO_2 , LiFePO_4) have been successfully used in commercial LIBs, a strong demand to improve their energy densities is awaiting the realization of the “next-generation” batteries operating at high voltage [12]. Spinel $\text{LiNi}_{0.5}\text{Mn}_{1.5}\text{O}_4$ (LNMO) has a better prospect as high energy density cathode material compared with currently used 4 V-class cathodes due to its high voltage plateau (ca. 4.7 V vs. Li^+/Li) and theoretical capacity (148 mAh g^{-1}) arising from the operation of $\text{Ni}^{2+}/\text{Ni}^{4+}$ redox couples.

Nevertheless, the high operating potential of $\text{LiNi}_{0.5}\text{Mn}_{1.5}\text{O}_4$ also leads to critical interface issues, such as electrolyte decomposition, high surface reactivity between the electrolyte and electrode, and gradual dissolution of Ni and Mn ions from the host structure. Especially, the dissolved transition metal ions can migrate through the electrolyte, which deposit on the surface of graphite and result in gradually decreased reversible capacity [6–10,13–18]. To solve this problem, extensive studies have been carried out to surface modification of cathode active materials with coating layer, including carbon materials, metals, oxides, phosphates, lithium compounds, polymers [19,20]. The coating layer could suppress the dissolution of Ni and Mn ions and decrease the oxidative decomposition of electrolyte on the surface of $\text{LiNi}_{0.5}\text{Mn}_{1.5}\text{O}_4$. However, the inorganic coating materials [21–27] (e.g. Al_2O_3 and ZrO_2) are usually not Li ion conductors, which will hinder Li ion diffusion between cathode active material and electrolyte. Furthermore, as the morphology of $\text{LiNi}_{0.5}\text{Mn}_{1.5}\text{O}_4$ is usually octahedron, the inorganic coating layer tends to be discontinuously deposited on the surface. Also, the complicated and high temperature treatment makes the coating process cost-effective and susceptible to ions interdiffusion between the inorganic coating layer and $\text{LiNi}_{0.5}\text{Mn}_{1.5}\text{O}_4$. In sharp contrast, the simple and low-cost polymer electrolyte conformal coating layer

* Corresponding authors.

E-mail addresses: zhangzy@qdu.edu.cn (Z. Zhang), cuiql@qibebt.ac.cn (G. Cui).

¹ These authors contributed equally to this work.

contributes to highly continuous surface coverage and fast Li ion transport [28–32]. These unique properties of polymer electrolyte coating will benefit for the enhanced $\text{LiNi}_{0.5}\text{Mn}_{1.5}\text{O}_4$ /electrolyte interface stability and capacity retention during long cycling.

In our previous study, a poly(ethyl α -cyanoacrylate) (PECA, formula as $(\text{CH}_2\text{C}(\text{CN})\text{COOC}_2\text{H}_5)_n$) based composite gel electrolyte was synthesized through an in-situ polymerization approach to improve the electrochemical performance of LiMn_2O_4 /graphite battery [33]. Owing to the strong interaction between cyano/ester groups of PECA and Li^+ , the dissociation of LiPF_6 was increased. As a result, the PECA gel electrolyte exhibited enhanced ionic conductivity in conventional organic electrolyte. On the other hand, the strong interaction energy of Mn^{2+} with cyano/ester groups made the PECA based electrolyte effectively suppress transition metallic ions transfer from the cathode to the counter graphite electrode, thus benefiting for the capacity retention during cycling. Moreover, the cyano-based polymer electrolyte exhibited high stability when it was applied in high potential $\text{LiNi}_{0.5}\text{Mn}_{1.5}\text{O}_4$ /Li batteries [34,35].

In this paper, PECA was explored for to modify the surface of spinel $\text{LiNi}_{0.5}\text{Mn}_{1.5}\text{O}_4$ particles via in-situ polymerization of ethyl α -cyanoacrylate (ECA). The conformal PECA polymer nano-coating layer could provide continuous surface coverage and lithium ion transport channel, which can guarantee the $\text{LiNi}_{0.5}\text{Mn}_{1.5}\text{O}_4$ /electrolyte interfacial stability and decrease the interface impedance. Moreover, the strong interaction energy of multivalent cations and PECA will suppress the dissolution of Ni and Mn ions from the host structure of $\text{LiNi}_{0.5}\text{Mn}_{1.5}\text{O}_4$ and avoid their deposition on the surface of anode. Therefore, in comparison to the pristine $\text{LiNi}_{0.5}\text{Mn}_{1.5}\text{O}_4$, the PECA-coated $\text{LiNi}_{0.5}\text{Mn}_{1.5}\text{O}_4$ exhibited superior cycling stability.

2. Experimental

2.1. Synthesis of PECA-coated $\text{LiNi}_{0.5}\text{Mn}_{1.5}\text{O}_4$

$\text{LiNi}_{0.5}\text{Mn}_{1.5}\text{O}_4$ was coated by PECA via an in-situ polymerization method. Firstly, diluted 8 mg of ethyl α -cyanoacrylate with 5 mL of anhydrous acetone. Secondly, 0.2 g of $\text{LiNi}_{0.5}\text{Mn}_{1.5}\text{O}_4$ commercial powder was dispersed in 30 mL of anhydrous acetone under continuous stirring and sonicated for 15 minutes. The diluted solution of ethyl α -cyanoacrylate was added dropwise to the $\text{LiNi}_{0.5}\text{Mn}_{1.5}\text{O}_4$ dispersion under magnetic stirring for approximately 1 hour in air. The moisture in air initiated the polymerization of ethyl α -cyanoacrylate on the surface of $\text{LiNi}_{0.5}\text{Mn}_{1.5}\text{O}_4$ particles. After sufficient polymerization reaction, the residual acetone was removed by rotary evaporation. Finally, the resulting powder of

PECA-coated $\text{LiNi}_{0.5}\text{Mn}_{1.5}\text{O}_4$ was dried at 80°C . The PECA-coated $\text{LiNi}_{0.5}\text{Mn}_{1.5}\text{O}_4$ was abbreviated to PECA-coated LNMO.

2.2. Samples characterization

The surface morphology and structure of the obtained materials were observed by field emission scanning electron microscopy (FE-SEM, Hitachi S-4800) and high resolution transmission electron microscopy (HRTEM, JEOL) with the magnifications from 10 k to 500 k. The crystallinity of pristine LNMO and PECA-LNMO powders was verified by X-ray diffraction (XRD, ADVANCED D8) in the range of 2-theta from 10° to 80° . Transmission Fourier transform infrared spectroscopy (FTIR) spectra were carried out using EO-SXB IR spectrometer in the wave number range of $400\text{--}2000\text{ cm}^{-1}$. The resolution used in FTIR was 4 cm^{-1} .

2.3. Electrochemical evaluation

The electrode was made by mixing 90 wt.% active material, 5 wt.% PVDF and 5 wt.% carbon black onto a Al current collector. All coin cells were assembled in an argon-filled glove box using Li metal as anode, Celgard 2300 as the separator, and 1.0 mol L^{-1} LiPF_6 dissolved in ethylene carbonate/dimethyl carbonate (EC:DMC = 1:1 v/v) as the electrolyte. The galvanostatic charge/discharge curves were tested on a LAND battery test system at varied C ($1\text{C} = 140\text{ mA g}^{-1}$) rates in the potential range of 3.5–5.0 V vs. Li/Li^+ at 25°C . The cyclic voltammetry (CV) curves were performed using a CHI 440 A instrument (CHI Instrument Inc.) with $\text{LiNi}_{0.5}\text{Mn}_{1.5}\text{O}_4$ or PECA-coated $\text{LiNi}_{0.5}\text{Mn}_{1.5}\text{O}_4$ as the working electrode and lithium metal as the counter and reference electrode in the potential range of 3.5–5.0 V vs. Li/Li^+ .

3. Results and discussion

The resultant products were characterized by XRD and FTIR to identify the crystal structure and composition, respectively. Fig. 1a shows the XRD patterns of the pristine and PECA-coated $\text{LiNi}_{0.5}\text{Mn}_{1.5}\text{O}_4$ powders. All patterns can be assigned to well-crystallized cubic spinel $\text{LiNi}_{0.5}\text{Mn}_{1.5}\text{O}_4$ (JCPDS Card No.: 80-2162, space group: $Fd\bar{3}m$), in which lithium ions occupy the tetrahedral (8a) sites and the transition metal ions (Mn and Ni) statistically reside at the octahedral (16d) site. The $\text{LiNi}_{0.5}\text{Mn}_{1.5}\text{O}_4$ powder coated with polymer molecule showed similar XRD patterns to that of pristine $\text{LiNi}_{0.5}\text{Mn}_{1.5}\text{O}_4$, indicating the polymer layer coating process did not alter the crystal structure of the $\text{LiNi}_{0.5}\text{Mn}_{1.5}\text{O}_4$ cathode [28]. The FTIR peaks (Fig. 1b) at about 1745 cm^{-1} (vs, $\text{C}=\text{O}$) and 1250 cm^{-1} (vs, $\text{C}-\text{O}$) could be attributed to the characteristic

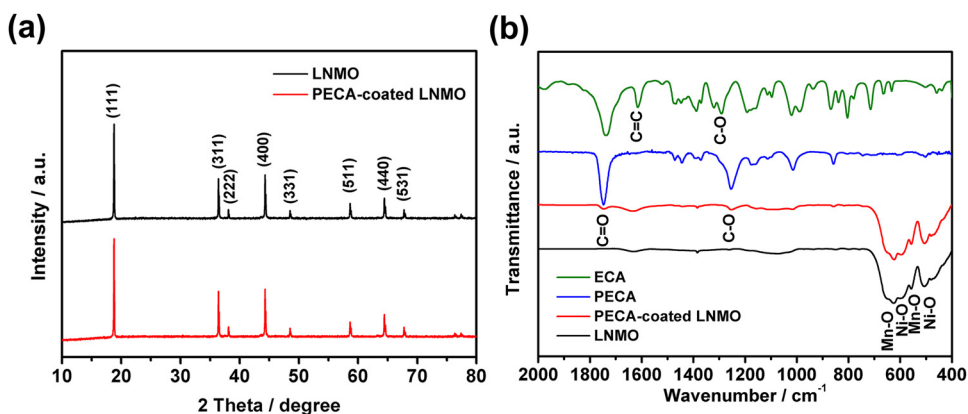


Fig. 1. (a) XRD patterns of the pristine and PECA-coated $\text{LiNi}_{0.5}\text{Mn}_{1.5}\text{O}_4$ powders. (b) FTIR spectra of the pristine $\text{LiNi}_{0.5}\text{Mn}_{1.5}\text{O}_4$ powder, PECA-coated $\text{LiNi}_{0.5}\text{Mn}_{1.5}\text{O}_4$ powder, PECA polymer, and ECA monomer.

absorption of PECA [36]. Compared with the FTIR spectrum of ECA monomer, the disappeared strong peak at 1618 cm^{-1} ($s, \text{C}=\text{C}$) of PECA polymer indicated the complete polymerization reaction initiated by moisture in air. In addition, the similar characteristic absorption peaks of PECA in pure PECA polymer and PECA-coated $\text{LiNi}_{0.5}\text{Mn}_{1.5}\text{O}_4$ suggested the PECA absorbed on the surface of $\text{LiNi}_{0.5}\text{Mn}_{1.5}\text{O}_4$ through surface hydrogen bonding. Furthermore, the peaks assigned to Mn-O (619 and 557 cm^{-1}) and Ni-O (588 and 496 cm^{-1}) showed no significant changes, demonstrating no distortion of the intrinsic lattice structure of $\text{LiNi}_{0.5}\text{Mn}_{1.5}\text{O}_4$ after PECA coating [37].

The surface morphology of the pristine and PECA-coated $\text{LiNi}_{0.5}\text{Mn}_{1.5}\text{O}_4$ was observed by SEM and HRTEM imaging. As shown in Fig. 2a and 2b, the pristine $\text{LiNi}_{0.5}\text{Mn}_{1.5}\text{O}_4$ particles exhibited a fine particulate morphology with smooth planes and well-defined edges. The average size of the pristine particles was $\sim 100\text{ nm}$. The morphology and size of the PECA-coated $\text{LiNi}_{0.5}\text{Mn}_{1.5}\text{O}_4$ particles (Fig. 2d and 2e) were consistent with that of the pristine sample. The HRTEM images (Fig. 2c and 2f) of $\text{LiNi}_{0.5}\text{Mn}_{1.5}\text{O}_4$ and PECA-coated $\text{LiNi}_{0.5}\text{Mn}_{1.5}\text{O}_4$ showed clear lattice fringes. The interplanar spacing was about 0.484 nm , which

corresponded to the (111) crystal plane of $\text{LiNi}_{0.5}\text{Mn}_{1.5}\text{O}_4$. This result was consistent with the XRD analyses and further confirmed no distortion of the intrinsic lattice structure after PECA coating. In addition, the HRTEM images also demonstrated the uniform and conformal coating of PECA layer on the surface of $\text{LiNi}_{0.5}\text{Mn}_{1.5}\text{O}_4$ particle with a thickness of approximately 10 nm , which was more uniform and continuous compared with conventional inorganic coatings [38]. The conformal coating layer can be favorable for protecting the whole $\text{LiNi}_{0.5}\text{Mn}_{1.5}\text{O}_4$ particle from electrolyte erosion during high voltage charging. As a result, the PECA coating layer is expected to enhance the electrochemical performance of $\text{LiNi}_{0.5}\text{Mn}_{1.5}\text{O}_4$ by providing a stable ionic conductive path and suppressing the interfacial decomposition reactions between electrolyte and electrode.

To investigate the cycling performance of $\text{LiNi}_{0.5}\text{Mn}_{1.5}\text{O}_4$ materials, $\text{LiNi}_{0.5}\text{Mn}_{1.5}\text{O}_4/\text{Li}$ half cells with 1.0 mol L^{-1} LiPF_6 EC/DMC (1:1 v/v) electrolyte without any additives were tested in the potential range of $3.5\text{--}5.0\text{ V}$. The charge/discharge profiles and capacity retention were shown in Fig. 3a and 3b. The long distinct plateau at around 4.7 V was corresponded to the $\text{Ni}^{2+/4+}$ redox couple of spinel $\text{LiNi}_{0.5}\text{Mn}_{1.5}\text{O}_4$, which agreed well with the pair of

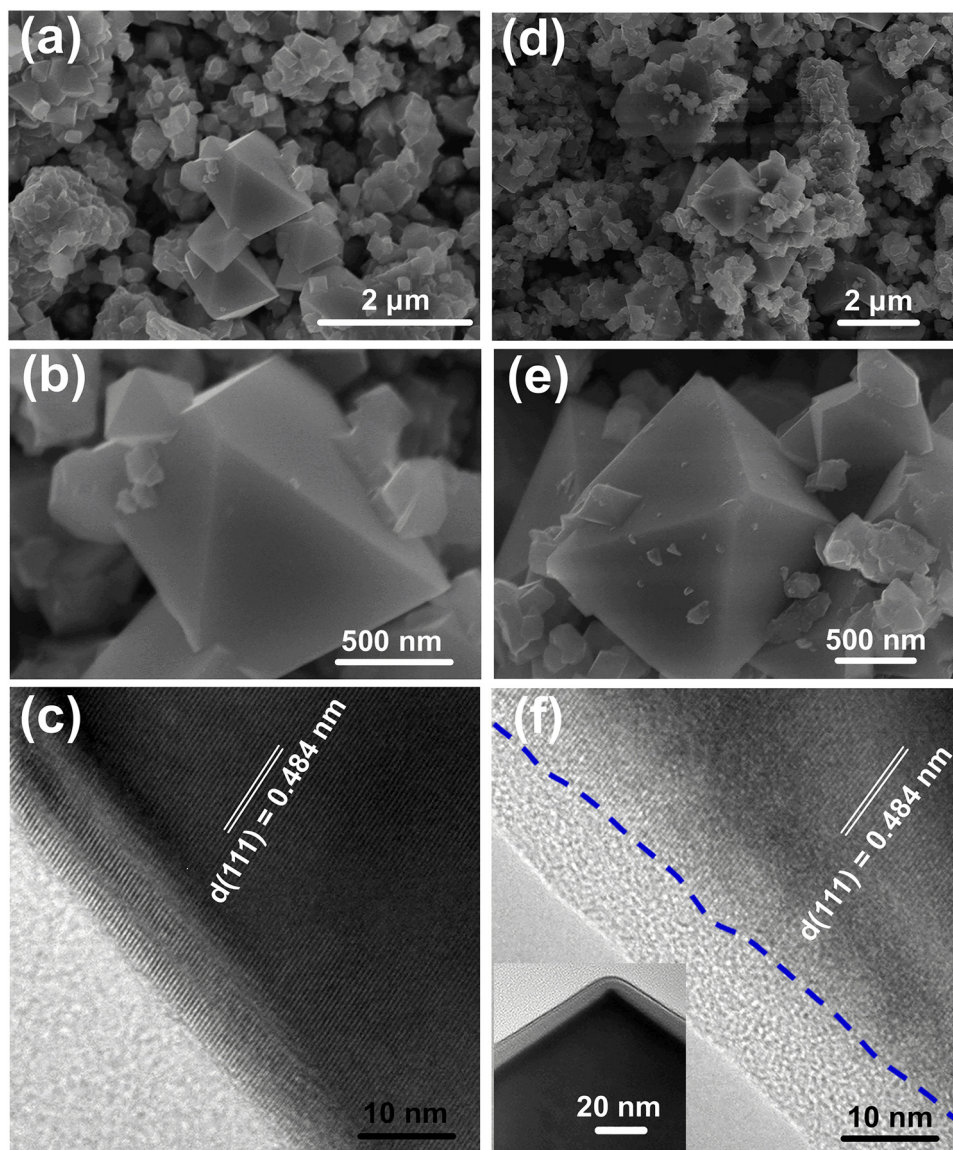


Fig. 2. Typical SEM and HRTEM images of the (a, b, c) pristine and (d, e, f) PECA-coated $\text{LiNi}_{0.5}\text{Mn}_{1.5}\text{O}_4$ (inset is a TEM image).

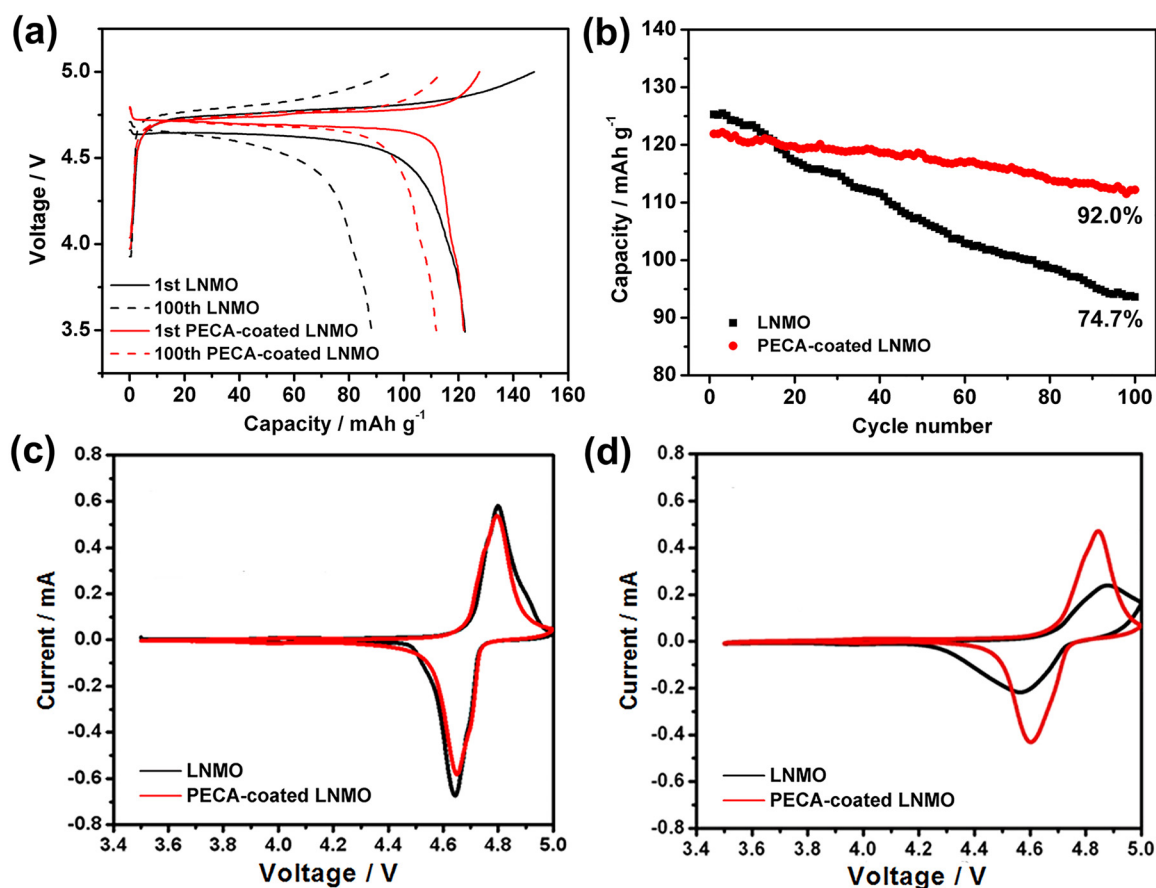


Fig. 3. (a) The initial and 100th charge and discharge curves of the pristine and PECA-coated $\text{LiNi}_{0.5}\text{Mn}_{1.5}\text{O}_4/\text{Li}$ cells at 1C. (b) Cycle performance of the pristine and PECA-coated $\text{LiNi}_{0.5}\text{Mn}_{1.5}\text{O}_4/\text{Li}$ cells at 1C. (c) Cyclic voltammograms of the pristine and PECA-coated $\text{LiNi}_{0.5}\text{Mn}_{1.5}\text{O}_4$ after the (c) 2nd and (d) 100th cycles at a scan rate of 0.2 mV s^{-1} in the voltage range of 3.5–5.0 V.

redox peaks in the cyclic voltammetry (CV) curves of $\text{LiNi}_{0.5}\text{Mn}_{1.5}\text{O}_4$ (Fig. 3c). The initial Coulombic efficiency of PECA-coated $\text{LiNi}_{0.5}\text{Mn}_{1.5}\text{O}_4$ was 95.4%, while that of the pristine $\text{LiNi}_{0.5}\text{Mn}_{1.5}\text{O}_4$ was only 85.3%. The larger capacity loss suggested worse interface side reactions happened in $\text{LiNi}_{0.5}\text{Mn}_{1.5}\text{O}_4/\text{Li}$ compared with the PECA-coated $\text{LiNi}_{0.5}\text{Mn}_{1.5}\text{O}_4/\text{Li}$ during the first charging and discharging. Furthermore, coating has been demonstrated as an effective strategy to reduce the polarization of $\text{LiNi}_{0.5}\text{Mn}_{1.5}\text{O}_4$ during cycling process, such as carbon coating reported by Yang et al. [19]. Here, for PECA-coated $\text{LiNi}_{0.5}\text{Mn}_{1.5}\text{O}_4$, there was little potential separation of charging-discharging plateaus and capacity fading between the initial cycle and the 100th cycle. By comparison, the pristine $\text{LiNi}_{0.5}\text{Mn}_{1.5}\text{O}_4$ exhibited larger variation in potential gap and severe capacity fading with the increasing cycling number, indicating the high polarization and poor cycle performance in $\text{LiNi}_{0.5}\text{Mn}_{1.5}\text{O}_4/\text{Li}$ cell. This result was consistent with CV curves of the pristine and PECA-coated $\text{LiNi}_{0.5}\text{Mn}_{1.5}\text{O}_4$ after the 2nd and 100th cycles (Fig. 3c and 3d). With cycle number increasing, the potential distance of peaks between anodic and cathodic (ΔV) increased, wherein a larger ΔV represents stronger electrode polarization. In the pristine $\text{LiNi}_{0.5}\text{Mn}_{1.5}\text{O}_4/\text{Li}$ cell, ΔV increased from 0.20 V to 0.33 V after the 100th cycle. In sharp comparison, the augmented ΔV was considerably retarded during cycling of the PECA-coated $\text{LiNi}_{0.5}\text{Mn}_{1.5}\text{O}_4/\text{Li}$ cell, where the corresponding ΔV varied from 0.20 V to 0.25 V. In addition, the peak area in the CV curves of $\text{LiNi}_{0.5}\text{Mn}_{1.5}\text{O}_4$ decreased much more seriously than that of PECA-

coated $\text{LiNi}_{0.5}\text{Mn}_{1.5}\text{O}_4$. It is known that liquid electrolytes are highly prone to electrochemical oxidation on the $\text{LiNi}_{0.5}\text{Mn}_{1.5}\text{O}_4$ surface at high voltage conditions, which has a detrimental influence on cycle performance. The significantly suppressed growth of ΔV as well as the retention of peak area in the PECA-coated $\text{LiNi}_{0.5}\text{Mn}_{1.5}\text{O}_4/\text{Li}$ cell confirmed the effectiveness of the PECA layer in preventing the formation of cathode-electrolyte interface layer, which hindered the charge transport at the $\text{LiNi}_{0.5}\text{Mn}_{1.5}\text{O}_4/\text{electrolyte}$ interface.

C-rate capability was also compared between the pristine and PECA-coated $\text{LiNi}_{0.5}\text{Mn}_{1.5}\text{O}_4$ with the charge-discharge current densities from 0.2C to 5.0C shown in Fig. 4a and 4b. Both electrodes exhibited the similar capacity from 0.2C to 5.0C. The capacity of PECA-coated $\text{LiNi}_{0.5}\text{Mn}_{1.5}\text{O}_4$ reached 70 mAh g^{-1} , which was slightly higher than that of the pristine $\text{LiNi}_{0.5}\text{Mn}_{1.5}\text{O}_4$. In our previous report [33], PECA was developed as gel polymer electrolyte, which exhibited high ionic conductivity of 0.33 mS cm^{-1} . This high ionic conductivity allowed for the fast ionic transport through the layer during high rate charging and discharging. The kinetic behavior of the cell based on pristine $\text{LiNi}_{0.5}\text{Mn}_{1.5}\text{O}_4$ and PECA-coated $\text{LiNi}_{0.5}\text{Mn}_{1.5}\text{O}_4$ was also investigated by CV techniques (Fig. 4c and 4d). The value of the apparent D_{Li} for PECA-coated $\text{LiNi}_{0.5}\text{Mn}_{1.5}\text{O}_4$ was calculated to be $1.27 \times 10^{-11} \text{ cm}^2 \text{ s}^{-1}$ according to the square root relationship between the peak current and the scan rate, as explained in previous report [39]. The value was the same order of magnitudes compared with that of the pristine $\text{LiNi}_{0.5}\text{Mn}_{1.5}\text{O}_4$ ($1.37 \times 10^{-11} \text{ cm}^2 \text{ s}^{-1}$). This result demonstrates that the PECA coating layer did not hamper the

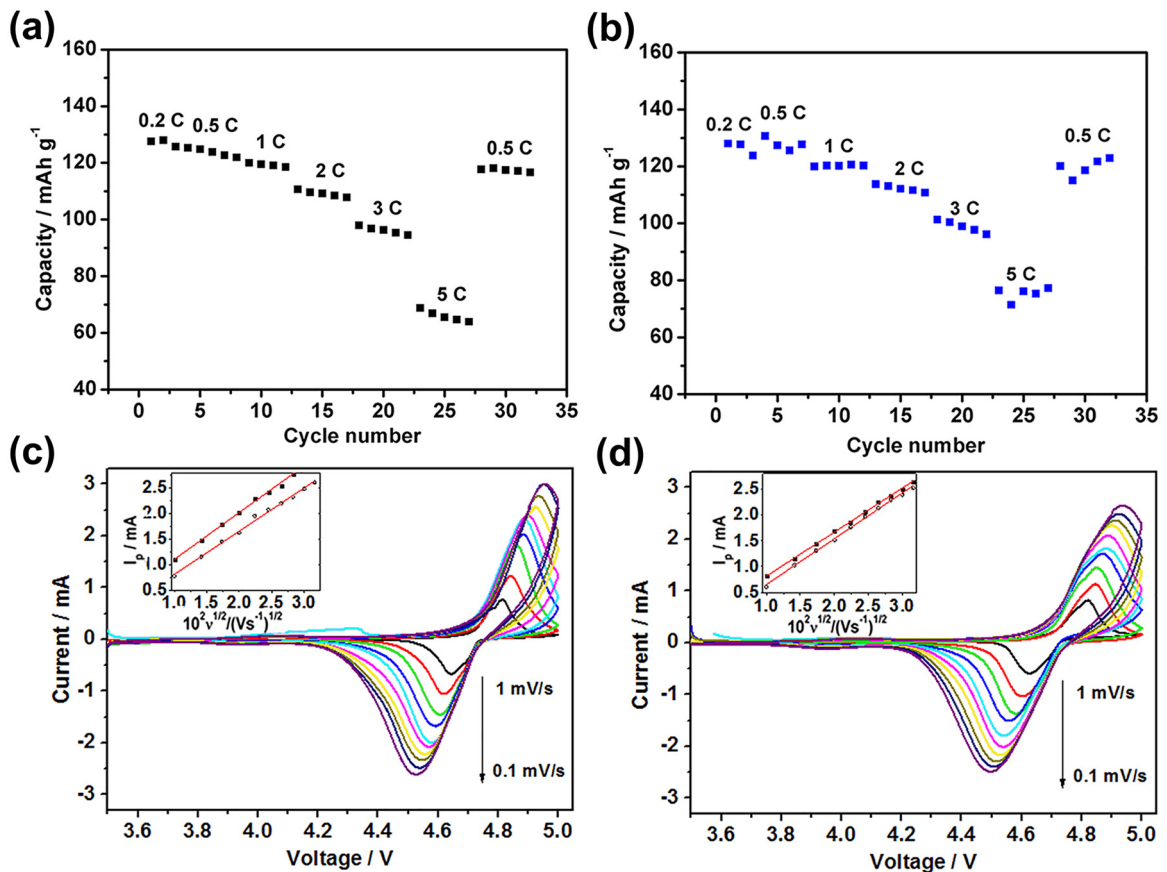


Fig. 4. Rate performance of the (a) pristine and (b) PECA-coated LiNi_{0.5}Mn_{1.5}O₄/Li cells. CV curves of the (c) pristine and (d) PECA-coated LiNi_{0.5}Mn_{1.5}O₄/Li cells at a series of sweep rates. Insets are the corresponding relationship between the peak current and the square root of sweep rate.

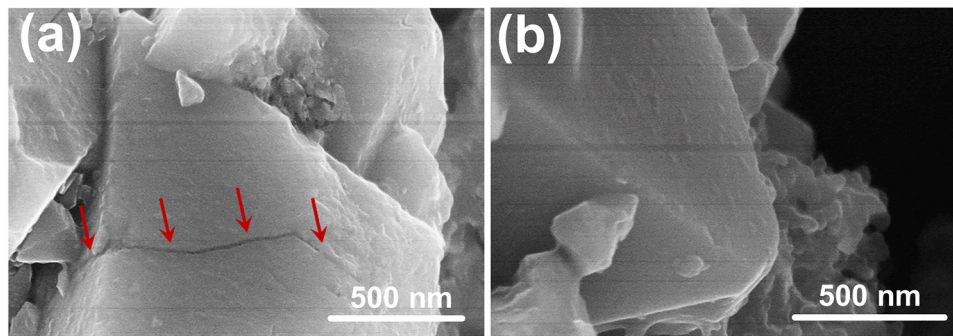


Fig. 5. Typical SEM images of the (a) pristine and (b) PECA-coated LiNi_{0.5}Mn_{1.5}O₄ electrodes after 100 cycles.

fast Li⁺ insertion/extraction between LiNi_{0.5}Mn_{1.5}O₄ and electrolyte during the cycling.

To further explain how the PECA coating layer ameliorates the cycling performance and restrains polarization of LiNi_{0.5}Mn_{1.5}O₄, the morphology changes of LiNi_{0.5}Mn_{1.5}O₄ electrodes after cycling were characterized. Fig. 5 showed the typical SEM images of the PECA-coated and uncoated LiNi_{0.5}Mn_{1.5}O₄ cathode electrodes after 100 charging and discharging cycles. For the uncoated LiNi_{0.5}Mn_{1.5}O₄, there were some cracks on the surface of active material particles, which could be explained by the well-known instability between naked LiNi_{0.5}Mn_{1.5}O₄ particles and organic electrolytes, as shown in Fig. 6. Though the cracks increased the contact area with the electrolyte and could have a beneficial effect on the Li⁺ ions transfer between active materials and electrolyte,

their destructions on the electron conduction between active materials was much severe to battery performance. These cracks destroyed the electronic contact among LiNi_{0.5}Mn_{1.5}O₄ particles and led to active LiNi_{0.5}Mn_{1.5}O₄ loss, which resulted in increasing interface impedance and capacity fading during battery cycling. Therefore, these cracks in LiNi_{0.5}Mn_{1.5}O₄ particles seem to be an incentive to bring about serious polarization and poor cycling performance. On the contrary, the PECA-coated LiNi_{0.5}Mn_{1.5}O₄ particles after 100 cycles showed a smooth surface similar to that prior to battery cycling, meaning that the influence of interface side reaction on the surface integrity was negligible. This unique property should be unambiguously ascribed to the protection of the conformal and highly continuous surface coverage by PECA nano-coating layer, which effectively suppressed the unexpected

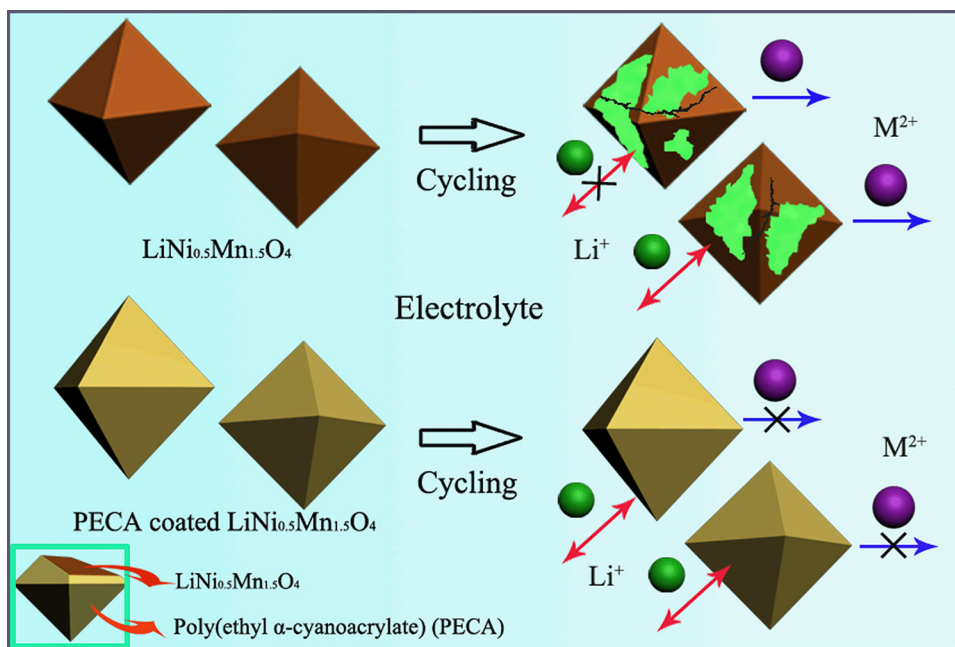


Fig. 6. Illustration for the influence of conformal PECA coating on the interface stability of $\text{LiNi}_{0.5}\text{Mn}_{1.5}\text{O}_4$.

side reaction between $\text{LiNi}_{0.5}\text{Mn}_{1.5}\text{O}_4$ particles and organic electrolytes. As a result, the particle integrity was maintained during cycling consequently enhanced capacity retention in PECA-coated $\text{LiNi}_{0.5}\text{Mn}_{1.5}\text{O}_4/\text{Li}$ cell.

4. Conclusions

The conformal nano-coating of PECA polymer electrolyte with the thickness of about 10 nm was explored to modify the high voltage interface stability of spinel $\text{LiNi}_{0.5}\text{Mn}_{1.5}\text{O}_4$ particles via in-situ polymerization of ethyl α -cyanoacrylate. The PECA coating layer with continuous coverage can provide facile ion transport and effectively suppress the unexpected side reaction at the interface between $\text{LiNi}_{0.5}\text{Mn}_{1.5}\text{O}_4$ and electrolyte. Therefore, in comparison to the pristine $\text{LiNi}_{0.5}\text{Mn}_{1.5}\text{O}_4$, the PECA-coated $\text{LiNi}_{0.5}\text{Mn}_{1.5}\text{O}_4$ showed remarkably decreased polarization and improved cycling performance. This work will shed light on the interface modification of $\text{LiNi}_{0.5}\text{Mn}_{1.5}\text{O}_4$ by reasonable application of high voltage polymer electrolyte materials in conventional LIBs.

Acknowledgements

This work was financially supported by the funding from “135” Projects Fund of CAS-QIBEBT Director Innovation Foundation, the Strategic Priority Research Program of the Chinese Academy of Sciences (Grant No. XDA09010105), Shandong Provincial Natural Science Foundation (Grant No. BS2015CL006, ZR2015BM002), National Natural Science Foundation of China (Grant No. 51502319), the Think-Tank Mutual Fund of Qingdao Energy Storage Industry Scientific Research, and Qingdao Key Lab of Solar Energy Utilization & Energy Storage Technology.

References

- [1] J.B. Goodenough, K.S. Park, The Li-ion rechargeable battery: a perspective, *J. Am. Chem. Soc.* 135 (2013) 1167.
- [2] M. Armand, J.-M. Tarascon, Issues and challenges for rechargeable lithium batteries, *Nature* 414 (2001) 9.
- [3] A. Ritchie, W. Howard, Recent developments and likely advances in lithium-ion batteries, *J. Power Sources* 162 (2006) 809.
- [4] B. Scrosati, J. Garche, Lithium batteries: Status, prospects and future, *J. Power Sources* 195 (2010) 2419.
- [5] A. Abouimrane, I. Belharouak, K. Amine, Sulfone-based electrolytes for high-voltage Li-ion batteries, *Electrochem. Commun.* 11 (2009) 1073.
- [6] K. Hayashi, Y. Nemoto, S.-i. Tobishima, J.-i. Yamaki, Mixed solvent electrolyte for high voltage lithium metal secondary cells, *Electrochim. Acta* 44 (1999) 2337.
- [7] M. Hu, X. Pang, Z. Zhou, Recent progress in high-voltage lithium ion batteries, *J. Power Sources* 237 (2013) 229.
- [8] Y. Watanabe, S.-i. Kinoshita, S. Wada, K. Hoshino, H. Morimoto, S.-i. Tobishima, Electrochemical properties and lithium ion solvation behavior of sulfone-ester mixed electrolytes for high-voltage rechargeable lithium cells, *J. Power Sources* 179 (2008) 770.
- [9] K. Xu, C.A. Angell, Sulfone-based electrolytes for lithium-ion batteries, *J. Electrochem. Soc.* 149 (2002) A920.
- [10] L. Xue, K. Ueno, S.-Y. Lee, C.A. Angell, Enhanced performance of sulfone-based electrolytes at lithium ion battery electrodes, including the $\text{LiNi}_{0.5}\text{Mn}_{1.5}\text{O}_4$ high voltage cathode, *J. Power Sources* 262 (2014) 123.
- [11] Z. Zhang, L. Hu, H. Wu, W. Weng, M. Koh, P.C. Redfern, L.A. Curtiss, K. Amine, Fluorinated electrolytes for 5 V lithium-ion battery chemistry, *Energy Environ. Sci.* 6 (2013) 1806.
- [12] M.S. Whittingham, Lithium batteries and cathode materials, *Chem. Rev.* 104 (2004) 32.
- [13] X. Cui, H. Zhang, S. Li, Y. Zhao, L. Mao, W. Zhao, Y. Li, X. Ye, Electrochemical performances of a novel high-voltage electrolyte based upon sulfolane and γ -butyrolactone, *J. Power Sources* 240 (2013) 476.
- [14] J. Demeaux, E. De Vito, D. Lemordant, M. Le Digabel, H. Galiano, M. Caillon-Caravanier, B. Claude-Montigny, On the limited performances of sulfone electrolytes towards the $\text{LiNi}_{0.4}\text{Mn}_{1.6}\text{O}_4$ spinel, *Phys. Chem. Chem. Phys.* 15 (2013) 20900.
- [15] S. Li, B. Li, X. Xu, X. Shi, Y. Zhao, L. Mao, X. Cui, Electrochemical performances of two kinds of electrolytes based on lithium bis(oxalate)borate and sulfolane for advanced lithium ion batteries, *J. Power Sources* 209 (2012) 295.
- [16] S. Li, Y. Zhao, X. Shi, B. Li, X. Xu, W. Zhao, X. Cui, Effect of sulfolane on the performance of lithium bis(oxalato)borate-based electrolytes for advanced lithium ion batteries, *Electrochim. Acta* 65 (2012) 221.
- [17] L. Mao, B. Li, X. Cui, Y. Zhao, X. Xu, X. Shi, S. Li, F. Li, Electrochemical performance of electrolytes based upon lithium bis(oxalato)borate and sulfolane/alkyl sulfite mixtures for high temperature lithium-ion batteries, *Electrochim. Acta* 79 (2012) 197.
- [18] J. Ma, P. Hu, G. Cui, L. Chen, Surface and interface issues in spinel $\text{LiNi}_{0.5}\text{Mn}_{1.5}\text{O}_4$: Insights into a potential cathode material for high energy density lithium ion batteries, *Chem. Mater.* 28 (2016) 3578.
- [19] W. Yang, H. Dang, S. Chen, H. Zou, Z. Liu, J. Lin, W. Lin, In situ carbon coated $\text{LiNi}_{0.5}\text{Mn}_{1.5}\text{O}_4$ cathode material prepared by prepolymer of melamine formaldehyde resin assisted method, *Int. J. Polym. Sci.* (2016) 4279457.
- [20] T.-F. Yi, J. Mei, Y.-R. Zhu, Key strategies for enhancing the cycling stability and rate capacity of $\text{LiNi}_{0.5}\text{Mn}_{1.5}\text{O}_4$ as high-voltage cathode materials for high power lithium-ion batteries, *J. Power Sources* 316 (2016) 85.

- [21] G. Alva, C. Kim, T. Yi, J.B. Cook, L. Xu, G.M. Nolis, J. Cabana, Surface chemistry consequences of Mg-based coatings on $\text{LiNi}_{0.5}\text{Mn}_{1.5}\text{O}_4$ electrode materials upon operation at high voltage, *J. Phys. Chem. C* 118 (2014) 10596.
- [22] Y. Fan, J. Wang, Z. Tang, W. He, J. Zhang, Effects of the nanostructured SiO_2 coating on the performance of $\text{LiNi}_{0.5}\text{Mn}_{1.5}\text{O}_4$ cathode materials for high-voltage Li-ion batteries, *Electrochim. Acta* 52 (2007) 3870.
- [23] J. Li, Y. Zhang, J. Li, L. Wang, X. He, J. Gao, AlF₃ coating of $\text{LiNi}_{0.5}\text{Mn}_{1.5}\text{O}_4$ for high-performance Li-ion batteries, *Ionics* 17 (2011) 671.
- [24] Y.K. Sun, K.J. Hong, J. Prakash, K. Amine, Electrochemical performance of nano-sized ZnO-coated $\text{LiNi}_{0.5}\text{Mn}_{1.5}\text{O}_4$ spinel as 5 V materials at elevated temperatures, *Electrochem. Commun* 4 (2002) 344.
- [25] Y.-K. Sun, Y.-S. Lee, M. Yoshio, K. Amine, Synthesis and electrochemical properties of ZnO-coated $\text{LiNi}_{0.5}\text{Mn}_{1.5}\text{O}_4$ spinel as 5 V cathode material for lithium secondary batteries, *Electrochem. Solid-State Lett* 5 (2002) A99.
- [26] H. Wang, T.A. Tan, P. Yang, M.O. Lai, L. Lu, High-rate performances of the R-doped spinel $\text{LiNi}_{0.5}\text{Mn}_{1.5}\text{O}_4$: Effects of doping and particle size, *J. Phys. Chem. C* 115 (2011) 6102.
- [27] T.-F. Yi, Y. Xie, M.-F. Ye, L.-J. Jiang, R.-S. Zhu, Y.-R. Zhu, Recent developments in the doping of $\text{LiNi}_{0.5}\text{Mn}_{1.5}\text{O}_4$ cathode material for 5 V lithium-ion batteries, *Ionics* 17 (2011) 383.
- [28] J.-H. Cho, J.-H. Park, M.-H. Lee, H.-K. Song, S.-Y. Lee, A polymer electrolyte-skinned active material strategy toward high-voltage lithium ion batteries: a polyimide-coated $\text{LiNi}_{0.5}\text{Mn}_{1.5}\text{O}_4$ spinel cathode material case, *Energy Environ. Sci* 5 (2012) 7124.
- [29] M.C. Kim, S.H. Kim, V. Aravindan, W.S. Kim, S.Y. Lee, Y.S. Lee, Ultrathin polyimide coating for a spinel $\text{LiNi}_{0.5}\text{Mn}_{1.5}\text{O}_4$ cathode and its superior lithium storage properties under elevated temperature conditions, *J. Electrochem. Soc* 160 (2013) A1003.
- [30] D. Lepage, C. Michot, G. Liang, M. Gauthier, S.B. Schougaard, A soft chemistry approach to coating of LiFePO_4 with a conducting polymer, *Angew. Chem. Int. Ed* 50 (2011) 6884.
- [31] C. Li, H.P. Zhang, L.J. Fu, H. Liu, Y.P. Wu, E. Rahm, R. Holze, H.Q. Wu, Cathode materials modified by surface coating for lithium ion batteries, *Electrochim. Acta* 51 (2006) 3872.
- [32] Y. Yang, G. Yu, J.J. Cha, H. Wu, M. Vosgueritchian, Y. Yao, Z. Bao, Y. Cui, Improving the performance of lithium-sulfur batteries by conductive polymer coating, *ACS Nano* 5 (2011) 9187.
- [33] P. Hu, Y. Duan, D. Hu, B. Qin, J. Zhang, Q. Wang, Z. Liu, G. Cui, L. Chen, Rigid-flexible coupling high ionic conductivity polymer electrolyte for an enhanced performance of $\text{LiMn}_2\text{O}_4/\text{graphite}$ battery at elevated temperature, *ACS Appl. Mater. Inter* 7 (2015) 4720.
- [34] J. Chai, J. Zhang, P. Hu, J. Ma, H. Du, L. Yue, J. Zhao, H. Wen, Z. Liu, G. Cui, L. Chen, A high-voltage poly(methylethyl α -cyanoacrylate) composite polymer electrolyte for 5 V lithium batteries, *J. Mater. Chem. A* 4 (2016) 5191.
- [35] P. Hu, J. Chai, Y. Duan, Z. Liu, G. Cui, L. Chen, Progress in nitrile-based polymer electrolytes for high performance lithium batteries, *J. Mater. Chem. A* 4 (2016) 10070.
- [36] Y. Zhou, F. Bei, H. Ji, X. Yang, L. Lu, X. Wang, Property and quantum chemical investigation of poly(ethyl α -cyanoacrylate), *J. Mol. Struct* 737 (2005) 117.
- [37] J.-H. Kim, A. Huq, M. Chi, N.P.W. Pieczonka, E. Lee, C.A. Bridges, M.M. Tessema, A. Manthiram, K.A. Persson, B.R. Powell, Integrated nano-domains of disordered and ordered spinel phases in $\text{LiNi}_{0.5}\text{Mn}_{1.5}\text{O}_4$ for Li-ion batteries, *Chem. Mater* 26 (2014) 4377.
- [38] H. Sun, B. Xia, W. Liu, G. Fang, J. Wu, H. Wang, R. Zhang, S. Kaneko, J. Zheng, H. Wang, D. Li, Significant improvement in performances of $\text{LiNi}_{0.5}\text{Mn}_{1.5}\text{O}_4$ through surface modification with high ordered Al-doped ZnO electro-conductive layer, *Appl. Surf. Sci* 331 (2015) 309.
- [39] T. Yang, N. Zhang, Y. Lang, K. Sun, Enhanced rate performance of carbon-coated $\text{LiNi}_{0.5}\text{Mn}_{1.5}\text{O}_4$ cathode material for lithium ion batteries, *Electrochim. Acta* 56 (2011) 4058.